



Porous metal micro-pillars by thermomechanical molding of two-phase alloys

Shweta Hanmant Jagdale, Golden Kumar *

Department of Mechanical Engineering, The University of Texas at Dallas, Richardson, TX 75080, USA



ARTICLE INFO

Article history:

Received 31 March 2023

Received in revised form 17 May 2023

Accepted 21 May 2023

Available online 22 May 2023

Keywords:

Thermomechanical molding

Creep

Porous microstructures

ABSTRACT

Creep-based thermomechanical molding of crystalline metals has emerged as a low-cost manufacturing technique for metal nanostructures. Here, we demonstrate the potential of such molding approach in fabrication of porous metal microstructures by using binary alloys such as Au-Si and Al-Cu. Two-phase alloys were isothermally molded against microscale templates followed by selective etching of one of the phases resulting in porous micro-pillars. The porosity of micro-pillars was varied by changing the phase fractions through alloy composition. Scanning electron microscopy is used to understand the different stages of molding and etching processes for two-phase metal alloys. While the nanoscale thermomechanical molding of similar alloys has been attributed to diffusional creep, the microscale forming presented here is dominated by the dislocation and grain boundary mediated deformation mechanisms. The molding and selective etching methodology can be potentially used to tailor the size and the distribution of pores by optimizing the microstructure of feedstock alloy.

© 2023 Elsevier B.V. All rights reserved.

1. Introduction

Metal nanostructures are of particular interest in catalytic [1,2], sensor [3], electrode [4], and biomedical [5,6] applications. Nano-manufacturing methods for metals are less advanced compared to polymers and semiconductors. Multiple lithographic and thin film deposition steps are needed even for fabrication of low aspect-ratio metal nanostructures. Solution based Polysol synthesis methods have become popular due to their ability to produce large quantities of high aspect-ratio metal nanowires and nanotubes [7,8]. However, the nanostructures grown in solution need to be subsequently dispersed and assembled for integration in devices which especially is challenging for high surface energy materials such as metals [9,10].

Low-cost molding of amorphous metals (also known as metallic glasses) in their supercooled viscous state has been significantly advanced at all length scales however the compositions are limited to glass forming alloys [11–16]. Recent breakthroughs in thermomechanical molding of crystalline metals provide inexpensive and versatile manufacturing technique for metallic nanostructures [17–19]. It has been shown that controllable nanostructures can be formed through diffusional creep by pressing a metal against templates at high homologous temperature [18]. Since the initial

discovery, numerous studies have been conducted to understand the flow mechanism during thermomechanical molding and advance the technique to a wide range of materials [19]. The molding capability has been demonstrated for metallic solid solutions [20], intermetallic compounds [21], semiconductors [19], and multi-element alloys [18]. Single crystalline metal nanostructures have also been formed by adjusting the orientation of starting material in molding [22]. Heterogeneous nanostructures were fabricated by harnessing the different diffusivity of elements and by engineering the mold-feedstock interface [20]. Latest work on molding of Au-Si alloys revealed that a small amount of Si can enhance the molding capability of Au-rich alloys by creating localized eutectic Au-Si interfaces even when the molding temperature is significantly lower than the melting temperature of the nominal alloy [23]. These studies clearly indicate that the flow of crystalline metals in nanoscale cavities is dominated by the interfacial diffusional creep. The diffusional creep is effective for molding of nanostructures, but fabrication of microscale or larger features is challenging by diffusion alone [19].

In this work, we use thermomechanical molding of two-phase alloys to fabricate microscale structures by utilizing the low melting temperature compositions. The superplastic deformation results in filling of mold cavities with two-phase alloys. Subsequently, one of the phases is selectively dissolved to generate porous metal micro-pillars. We use Au-Si and Al-Cu alloys to demonstrate that

* Corresponding author.

E-mail address: Golden.Kumar@UTDallas.edu (G. Kumar).

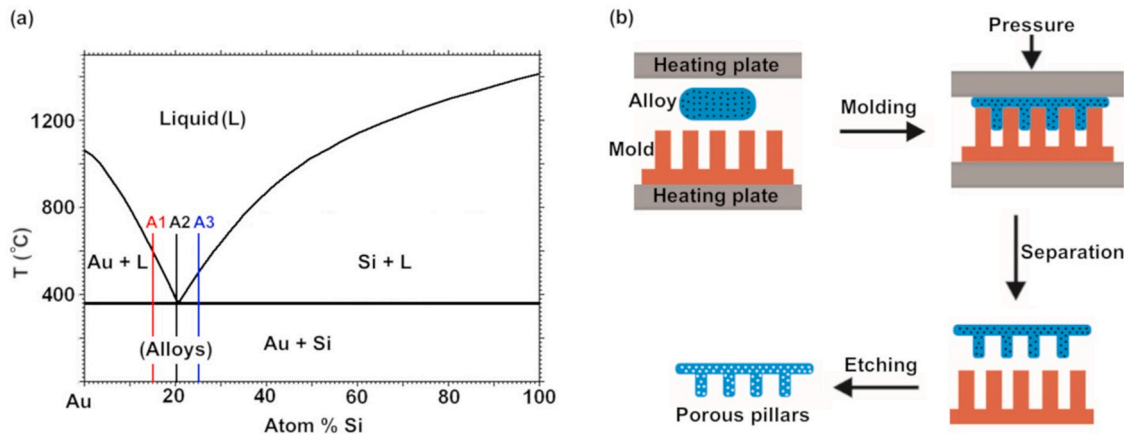


Fig. 1. (a) Au-Si phase diagram showing the three compositions (A1, A2, and A3) studied in this work. (b) Schematic illustration of thermomechanical molding and etching scheme used to fabricate porous metal micro-pillars.

microscale structures with varying porosity are feasible by combination of thermomechanical molding and selective etching.

2. Material and methods

Au-Si (Au₈₅Si₁₅, Au₈₀Si₂₀, and Au₇₅Si₂₅) and Al-Cu (Al₅₀Cu₅₀) alloys were prepared by melting 99.9% pure elements in a quartz tube under argon atmosphere. Cylindrical rods with diameters of about 2 mm were produced by rapid cooling to form fine microstructure. The as-prepared samples were characterized using TA Instruments 25 P differential scanning calorimeter (DSC) to compare the melting temperatures with the values estimated from the corresponding phase diagrams. The microstructure and the composition of alloys were characterized using scanning electron microscopy (SEM) and energy-dispersive x-ray spectroscopy (EDS).

Thermomechanical molding experiments were conducted in air using custom-made heating plates installed on Instron mechanical testing machine with a 50 kN load cell. Small pieces of as-prepared alloys were deformed into discs of 5 mm diameter by pressing between the heated plates. The discs were polished to about 500 μm thickness and used as the feedstock for molding experiments. Thermomechanical molding conditions were optimized by systematic variation in temperature, load, and time. The molding capability of alloys was proportional to the homologous temperatures. The data presented here correspond to the optimal molding temperatures of 320 °C and 425 °C for Au-Si and Al-Cu alloys, respectively.

Si molds with 5–20 μm diameter cavities and nanoporous alumina with 250 nm diameter pores were used as the templates for microscale and nanoscale molding experiments, respectively. The Si molds were prepared by photolithography and deep-reactive ion

etching and the Whatman™ alumina molds were acquired from Millipore SiGMA. Both Si and alumina templates were etched away in 60 wt% KOH solution at 90 °C and the released metal structures were characterized by Zeiss Supra 40 SEM. In addition to the etching of the templates, KOH also selectively removed Si from Au-Si alloys and Al from Al-Cu alloy resulting in formation of porous Au and Cu structures. The etching was stopped when the bubble formation due to exothermic reaction ceased, which was less than 30 min for both alloy systems.

3. Results and discussion

Fig. 1 shows the schematic illustration of thermomechanical molding and selective etching scheme used for fabrication of porous metal microstructures using an example of Au-Si eutectic system. Au-Si phase diagram displays deep eutectic at about 20 at% Si with a melting temperature of 364 °C. The Au-Si alloys have been extensively studied for growth of Si nanowires [24,25]. The Au-Si alloys around eutectic solidify into fine microstructure consisting of Au and Si phases with limited solid solubility [26]. We hypothesize the use of two-phase eutectic morphology to produce porous structures as depicted in **Fig. 1b**. The alloys such as Au-Si are expected to retain the dual phase microstructure when pressed against a mold at high homologous temperatures if the mold size is larger than the microstructural features. After separating the samples from the mold, one phase can be selectively etched out resulting in porous metal geometries defined by the mold. The porosity of metal structures can be varied by adjusting the fraction of soluble phase through selection of alloy composition. For example, three compositions Au₈₅Si₁₅ (A1), Au₈₀Si₂₀ (A2), and Au₇₅Si₂₅ (A3) marked in **Fig. 1** are envisioned to yield varying porosity because of different fraction of Si phases.

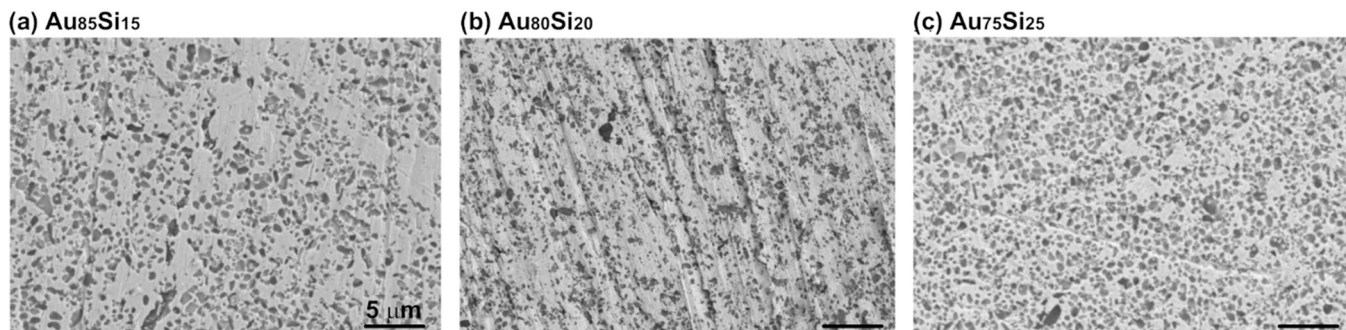


Fig. 2. The SEM images of discs made by pressing of (a) Au₈₅Si₁₅, (b) Au₈₀Si₂₀, and (c) Au₇₅Si₂₅ alloys. The dark particles are Si and the remaining matrix is Au.

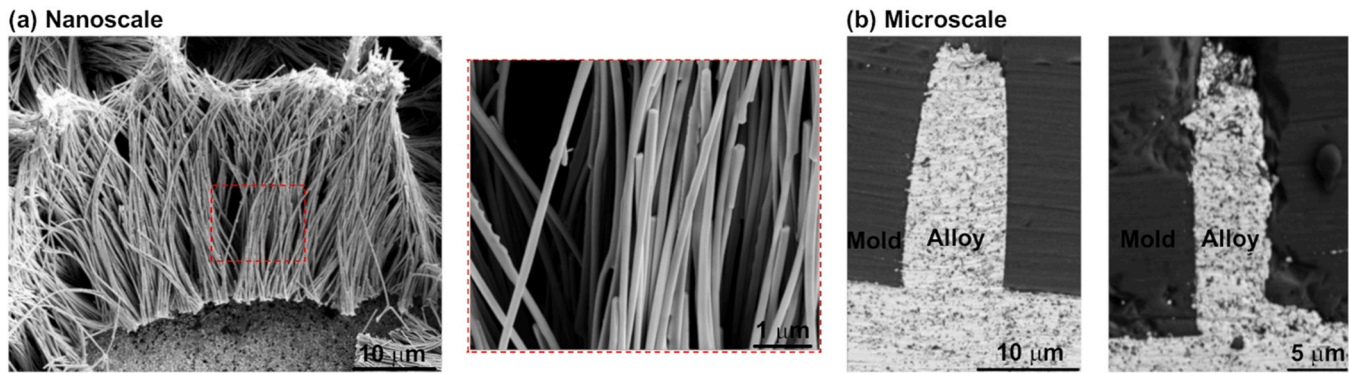


Fig. 3. Thermomechanical molding of $\text{Au}_{80}\text{Si}_{20}$ using nanoscale and microscale molds. (a) SEM image of Au nanowires formed during nanomolding due to diffusion dominated flow. (b) SEM images of $10\text{ }\mu\text{m}$ and $5\text{ }\mu\text{m}$ diameter pillars with nominal alloy composition formed by microscale molding.

The thermomechanical molding mechanism depends on the microstructure of the feedstock material and the size of the mold [18]. Fig. 2 shows the SEM images of three Au-Si discs used as the feedstock in present work. The SEM images and the EDX analysis reveal that all three samples consist of sub-micron sized cuboidal Si particles embedded in continuous Au matrix. According to Au-Si equilibrium phase diagram, small fraction of primary Au or Si phases is expected along with eutectic microstructure for off-eutectic compositions. However, the rapid cooling used here prevents the formation of large primary phases. The volume fraction of Si phase in three discs was estimated from the image analysis by using 4–5 images taken at different locations to obtain average values. These estimated values are 28.1%, 29.7%, and 36.9% for A1, A2, and A3 alloys, respectively. The measured values of Si volume fraction at the disc surface are higher than the values calculated from the weight fractions and the densities of Au and Si. The Si enrichment on the surface of Au-Si discs is likely due to pressure induced diffusion of Si during flat disc formation at high temperature. Previous study has shown accumulation of Si on the surface of Au-Si feedstock due to diffusion caused by pressure gradient during molding [23]. The ability to alter the microstructure of feedstock by pre-pressing can serve as an additional control parameter in thermomechanical molding of alloys.

To understand the effect of microstructure and mold size on thermomechanical forming, the Au-Si alloys were pressed against 250 nm diameter alumina and 5–10 μm diameter Si molds. The nanoscale and microscale molding experiments were conducted at 320 °C for 3 min under 5000 N and 1500 N, respectively. Fig. 3 shows the SEM images of $\text{Au}_{80}\text{Si}_{20}$ alloy subjected to nanoscale and microscale molding. Nanoscale molding results in formation of high-aspect ratio (> 100) nanowires (Fig. 3a), which are predominantly Au as indicated by the EDX analysis. A significant change compared to the nominal composition is expected because the microstructural features of $\text{Au}_{80}\text{Si}_{20}$ alloy are larger than the mold cavities. It has been reported that the thermomechanical nanomolding of crystalline metals is controlled by the interfacial diffusion and the final composition depends on the diffusivity of constituent elements [18,20]. The previous molding work on Au-Si showed the formation of core (Au)-shell (Si) nanowires but the use of KOH for mold removal can dissolve the Si shell resulting in pure Au nanowires [23]. Therefore, the molding of alloy nanostructures with feedstock composition requires comparable diffusivity of constituent elements such as Au and Ag [20]. The diffusivity of Si is about two orders of magnitude smaller than the diffusivity of Au in Au-Si [23].

In the case of microscale molding experiments, the $\text{Au}_{80}\text{Si}_{20}$ alloy was not removed from the Si molds after pressing to prevent the etching of Si from the molded features. The cross-section of mold-

alloy stack was mechanically polished to expose the side view of filled cavities as shown in Fig. 3b. Both Au and Si phases are clearly observed in the SEM images of $10\text{ }\mu\text{m}$ and $5\text{ }\mu\text{m}$ cavities and the overall microstructure remains similar to the feedstock discs which are also visible in the lower part of the images (Fig. 3b). The EDX analysis confirmed that the Au-Si composition in the microscale cavities resembles with the nominal alloy composition. No significant change in the size of Si particles is observed during molding. Similar results were obtained for $\text{Au}_{85}\text{Si}_{15}$ and $\text{Au}_{75}\text{Si}_{25}$ alloys. The ability to fill the microscale cavities with uniform two-phase Au-Si alloys suggests that interfacial diffusion is not the dominant molding mechanism as in the previous studies on nanoscale molding [9]. It is mainly the diffusion assisted grain boundary sliding and dislocation mediated deformation which are used in large scale superplastic forming of ultrafine grain crystalline metals [27,28]. The transition between the different deformation mechanisms is controlled by the size of microstructural features and the mold cavity [18]. The present findings show that two-phase alloys can be molded while retaining the microstructure and the composition if the mold size is larger than the microstructural components.

The presence of two phases in microscale features can be utilized to fabricate porous microstructure by selective etching of one of the phases. Si was dissolved from Au-Si alloys using KOH. Fig. 4 shows the SEM images of $10\text{ }\mu\text{m}$ diameter porous pillars of three Au-Si alloys made by molding and selective etching. The porosity levels estimated from the images are consistent with the microstructure of the feedstock materials. Majority of the pillars retained the geometric integrity after selective etching however some pillars collapsed due to thermal stress and high porosity levels. The thermal stress was improved by slow cooling, but the porosity induced collapsing was still evident in highly porous micro-pillars. Si was removed from the surface of micro-pillars however some residual Si can be present in interior which was not accessible to the etchant.

The issue of residual phase can be mitigated by first selectively etching the surface of feedstock disc followed by thermomechanical molding (Fig. 5). Fig. 5a shows the SEM image of $\text{Au}_{80}\text{Si}_{20}$ disc after etching in KOH until all the Si from surface layer was etched. Subsequently, the partially etched disc was pressed against $5\text{ }\mu\text{m}$ diameter cavities in Si by placing the porous side on the Si. After molding, the samples were submerged in KOH to separate from the mold and remove any remaining Si from the pillars. As shown in Fig. 5b, an array of porous Au micro-pillars formed which remained largely vertical. The higher magnification SEM image reveals the presence of pores throughout the length of the pillars. We believe the etching followed by molding approach produces better quality porous structures free of any remaining second phase. Partial etching helps in retaining the low melting temperature required for superplastic forming.

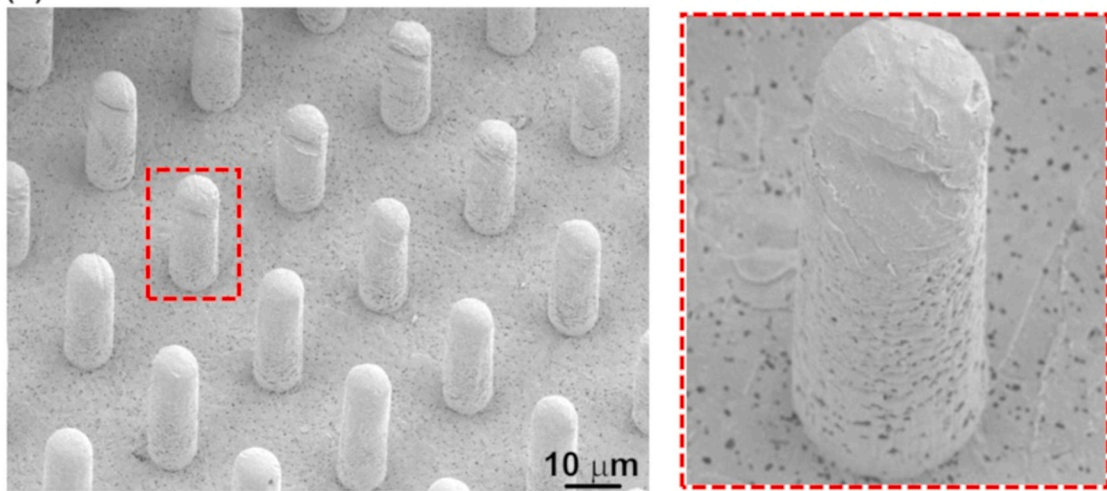
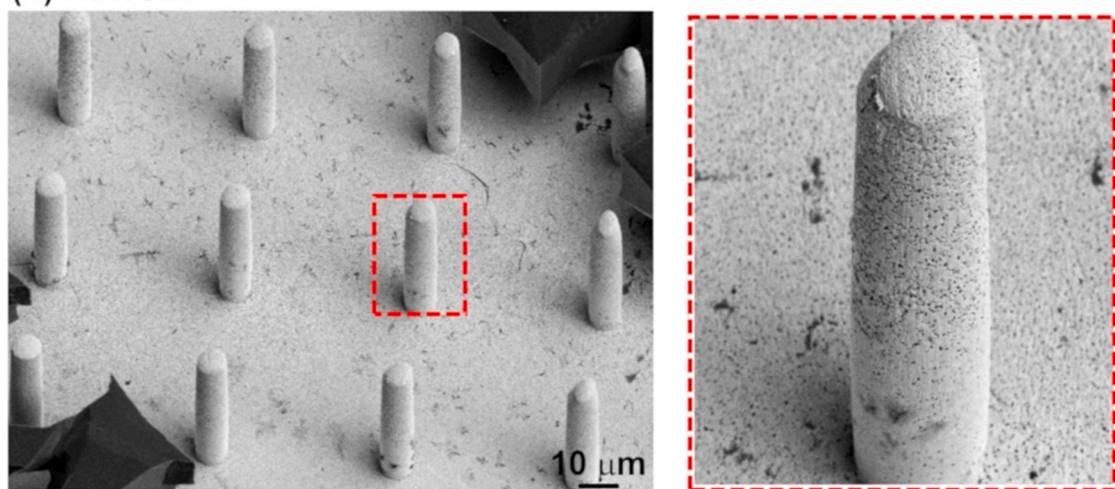
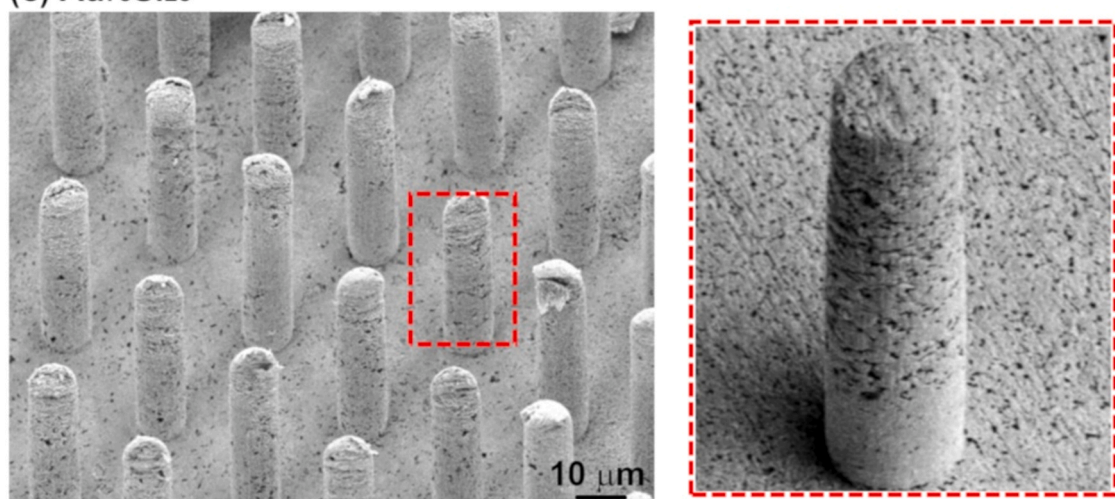
(a) $\text{Au}_{85}\text{Si}_{15}$ (b) $\text{Au}_{80}\text{Si}_{20}$ (c) $\text{Au}_{75}\text{Si}_{25}$ 

Fig. 4. Porous pillars with diameters of 10 μm fabricated by thermomechanical molding and selective etching of (a) $\text{Au}_{85}\text{Si}_{15}$, (b) $\text{Au}_{80}\text{Si}_{20}$, and (c) $\text{Au}_{75}\text{Si}_{25}$ alloys.

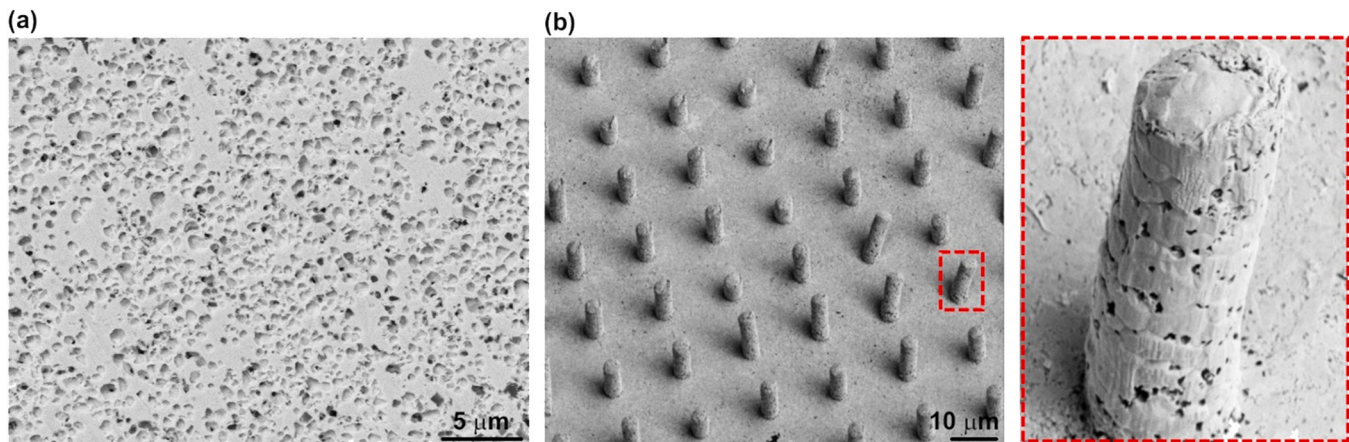


Fig. 5. (a) SEM image of $\text{Au}_{80}\text{Si}_{20}$ disc after prolonged etching in KOH. (b) Porous micro-pillars formed by molding the pre-etched disc (shown in 5a) against 5 μm diameter cavities.

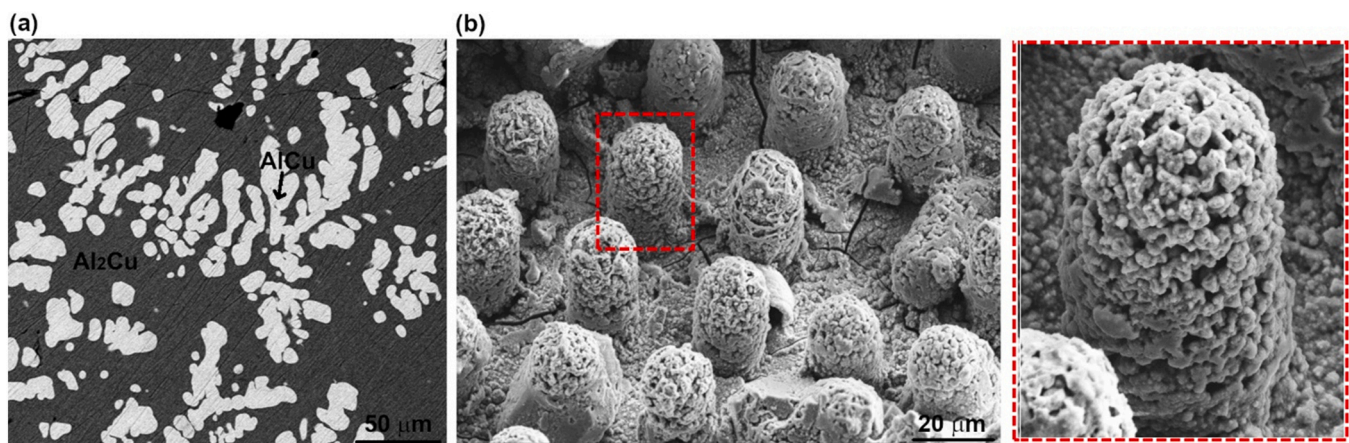


Fig. 6. (a) SEM image of as-prepared $\text{Al}_{50}\text{Cu}_{50}$ sample. (b) Porous Cu micro-pillars formed by thermomechanical molding and subsequent etching of Al.

To test the applicability of proposed methodology to other two-phase alloy systems, $\text{Al}_{50}\text{Cu}_{50}$ alloy was investigated. Fig. 6a shows an SEM image of as-prepared $\text{Al}_{50}\text{Cu}_{50}$ alloy revealing the presence of dendritic AlCu (η_2) phase embedded in Al_2Cu (θ) matrix. The Al-Cu disc was pressed against 20 μm diameter cavities at 425 $^{\circ}\text{C}$ under 5000 N for 3 min followed by selective etching of Al using KOH. Porous Cu micro-pillars were formed as shown in Fig. 6b and the corresponding higher magnification image. However, $\text{Al}_{50}\text{Cu}_{50}$ alloy did not deform homogeneously like the Au-Si alloys due to high melting temperature of $\text{Al}_{50}\text{Cu}_{50}$ alloy and the presence of hard intermetallic phases. The dominant monoclinic η_2 phase is known to be the hardest phase among all Al-Cu intermetallics with hardness values in the range of 9–10 GPa [29]. It is likely that the softer θ phase (hardness \sim 6–7 GPa) deformed and predominantly filled the mold cavities. Porous Cu pillars are generated irrespective of the deforming phase because Al is present in both phases. Coarse ($>20\text{ }\mu\text{m}$) η_2 dendrites further prevented the homogeneous flow of two-phase Al-Cu alloys resulting in inferior molding capability. In contrast, fine ($<1\text{ }\mu\text{m}$) equiaxed hard Si particles in Au-Si alloys do not significantly hinder the flow of soft Au matrix (hardness \sim 1–1.5 GPa). Therefore, the geometry and the hardness of constituent phases are critical for successful thermomechanical molding of crystalline metals.

In Al-Cu alloys, Al-rich compositions are more suitable for thermomechanical molding due to the presence of soft Al phase and the low melting temperature. We performed initial molding and selective etching experiments on $\text{Al}_{83}\text{Cu}_{17}$ alloy but the resulting porous

Cu micropillars were not mechanically stable when large volume fraction of Al was etched out. More research is needed to select the suitable combination of alloy composition and etching technique to form durable porous microstructures.

4. Conclusions

We investigated the thermomechanical molding of dual phase Au-Si and Al-Cu crystalline alloys. The results show that the mechanism of molding of two-phase alloys depends on the size, the shape, and the mechanical properties of the constituent phases. Interfacial diffusional creep dominates when the mold size is smaller than the microstructural features as in the cases of extensively studied nanomolding. Under such conditions, the composition of molded nanostructure deviates from the feedstock alloy due to different diffusivity values. Nanoscale molding of three different Au-Si compositions resulted in formation of only Au nanowires because of higher diffusivity of Au than Si. The absence of Si in nanowires can also be due to use of KOH for mold removal which may have etched any Si present. The two-phase morphology can be retained in during thermomechanical molding when the microstructural features in the feedstock material are significantly smaller than the mold size. Superplastic forming through grain-boundary sliding and dislocation slip and glide results in homogenous filling of mold cavities with two-phase mixture. This finding provides unique opportunity to achieve porous structures by chemically removing one of the phases. The proof-of-concept is demonstrated by fabricating porous Au and Cu micro-pillars by

thermomechanical molding and etching of Au-Si and Al-Cu alloys, respectively. Thermomechanical molding is more suitable for alloys consisting of low hardness phases with fine microstructure. More research is required to explore the full potential of the proposed approach.

CRediT authorship contribution statement

Shweta Jagdale: Methodology, Formal analysis, Writing – original draft. **Golden Kumar:** Conceptualization, Supervision, Writing – review & editing, Funding acquisition.

Data availability

Data will be made available on request.

Declaration of Competing Interest

The authors declare that they have no known competing financial interests or personal relationships that could have appeared to influence the work reported in this paper.

Acknowledgements

The work was supported by the National Science Foundation (NSF) through CMMI Award#2212195.

References

- [1] B. Lim, M.J. Jiang, T. Yu, P.H.C. Camargo, Y.N. Xia, Nucleation and growth mechanisms for Pd-Pt bimetallic nanodendrites and their electrocatalytic properties, *Nano Res.* 3 (2010) 69–80.
- [2] Y.G. Sun, B. Mayers, Y.N. Xia, Metal nanostructures with hollow interiors, *Adv. Mater.* 15 (2003) 641–646.
- [3] A.N. Shipway, E. Katz, I. Willner, Nanoparticle arrays on surfaces for electronic, optical, and sensor applications, *Chem. Phys. Chem.* 1 (2000) 18–52.
- [4] D.S. Hecht, L.B. Hu, G. Irvin, Emerging transparent electrodes based on thin films of carbon nanotubes, graphene, and metallic nanostructures, *Adv. Mater.* 23 (2011) 1482–1513.
- [5] M. Hu, J.Y. Chen, Z.Y. Li, L. Au, G.V. Hartland, X.D. Li, M. Marquez, Y.N. Xia, Gold nanostructures: engineering their plasmonic properties for biomedical applications, *Chem. Soc. Rev.* 35 (2006) 1084–1094.
- [6] L. Au, D.S. Zheng, F. Zhou, Z.Y. Li, X.D. Li, Y.N. Xia, A quantitative study on the photothermal effect of immuno gold nanocages targeted to breast cancer cells, *ACS Nano* 2 (2008) 1645–1652.
- [7] Y.N. Xia, P.D. Yang, Y.G. Sun, Y.Y. Wu, B. Mayers, B. Gates, Y.D. Yin, F. Kim, Y.Q. Yan, One-dimensional nanostructures: Synthesis, characterization, and applications, *Adv. Mater.* 15 (2003) 353–389.
- [8] B. Wiley, Y.G. Sun, J.Y. Chen, H. Cang, Z.Y. Li, X.D. Li, Y.N. Xia, Shape-controlled synthesis of silver and gold nanostructures, *MRS Bull.* 30 (2005) 356–361.
- [9] K.J.M. Bishop, C.E. Wilmer, S. Soh, B.A. Grzybowski, Nanoscale forces and their uses in self-assembly, *Small* 5 (2009) 1600–1630.
- [10] J.C. Love, A.R. Urbach, M.G. Prentiss, G.M. Whitesides, Three-dimensional self-assembly of metallic rods with submicron diameters using magnetic interactions, *J. Am. Chem. Soc.* 125 (2003) 12696–12697.
- [11] G. Kumar, H.X. Tang, J. Schroers, Nanomoulding with amorphous metals, *Nature* 457 (2009) 868–872.
- [12] G. Kumar, A. Desai, J. Schroers, Bulk metallic glass: the smaller the better, *Adv. Mater.* 23 (2011) 461–476.
- [13] M. Kanik, P. Bordeennithikasem, G. Kumar, E. Kinser, J. Schroers, High quality factor metallic glass cantilevers with tunable mechanical properties, *Appl. Phys. Lett.* 105 (2014) 131911.
- [14] Y. Saotome, K. Imai, S. Shioda, S. Shimizu, T. Zhang, A. Inoue, The micro-nano-formability of Pt-based metallic glass and the nanoforming of three-dimensional structures, *Intermetallics* 10 (2002) 1241–1247.
- [15] M. Hasan, N. Kahler, G. Kumar, Shape-controlled metal-metal and metal-polymer janus structures by thermoplastic embossing, *Acs Appl. Mater. Inter.* 8 (2016) 11084–11090.
- [16] M. Hasan, J. Schroers, G. Kumar, Functionalization of metallic glasses through hierarchical patterning, *Nano Lett.* 15 (2015) 963–968.
- [17] Z. Liu, One-step fabrication of crystalline metal nanostructures by direct nanoimprinting below melting temperatures, *Nat. Commun.* 8 (2017) 7.
- [18] Z. Liu, N.J. Liu, J. Schroers, Nanofabrication through molding, *Prog. Mater. Sci.* 125 (2022) 43.
- [19] Z. Liu, G.X. Han, S. Sohn, N.J. Liu, J. Schroers, Nanomolding of crystalline metals: the smaller the easier, *Phys. Rev. Lett.* 122 (2019) 036101.
- [20] N.J. Liu, G.N. Liu, A. Raj, S. Sohn, M.D. Morales-Acosta, J.B. Liu, J. Schroers, Unleashing nanofabrication through thermomechanical nanomolding, *Sci. Adv.* 7 (2021) 1–7.
- [21] N.J. Liu, Y.J. Xie, G.N. Liu, S. Sohn, A. Raj, G.X. Han, B.Z. Wu, J.J. Cha, Z. Liu, J. Schroers, General nanomolding of ordered phases, *Phys. Rev. Lett.* 124 (2020) 036102.
- [22] G.N. Liu, S. Sohn, N.J. Liu, A. Raj, U.D. Schwarz, J. Schroers, Single-crystal nanostructure arrays forming epitaxially through thermomechanical nanomolding, *Nano Lett.* 21 (2021) 10054–10061.
- [23] A. Raj, N.J. Liu, G.N. Liu, S. Sohn, J.X. Xiang, Z. Liu, J. Schroers, Nanomolding of gold and gold-silicon heterostructures at room temperature, *ACS Nano* 15 (2021) 14275–14284.
- [24] J.B. Hannon, S. Kodambaka, F.M. Ross, R.M. Tromp, The influence of the surface migration of gold on the growth of silicon nanowires, *Nature* 440 (2006) 69–71.
- [25] S. Hofmann, R. Sharma, C.T. Wirth, F. Cervantes-Sodi, C. Ducati, T. Kasama, R.E. Dunin-Borkowski, J. Drucker, P. Bennett, J. Robertson, Ledge-flow-controlled catalyst interface dynamics during Si nanowire growth, *Nat. Mater.* 7 (2008) 372–375.
- [26] S. Hassam, J. Agren, M. Gauneescard, J.P. Bros, T.H.E. AG-AU-Si, System - experimental and calculated phase-diagram, *Metall. Mater. Trans. A* 21 (1990) 1877–1884.
- [27] M. Kawasaki, T.G. Langdon, Principles of superplasticity in ultrafine-grained materials, *J. Mater. Sci.* 42 (2007) 1782–1796.
- [28] Y. Ma, M. Furukawa, Z. Horita, M. Nemoto, R.Z. Valiev, T.G. Langdon, Significance of microstructural control for superplastic deformation and forming, *Mater. Trans. JIM* 37 (1996) 336–339.
- [29] Y. Xiao, H. Besharatloo, B. Gan, X. Maeder, R. Spolenak, J.M. Wheeler, Combinatorial investigation of Al-Cu intermetallics using small-scale mechanical testing, *J. Alloy. Comp.* 822 (2020) 153536.